Chapter 8
Recurrence Analysis of Otoacoustic Emissions

Giovanna Zimatore and Marta Cavagnaro

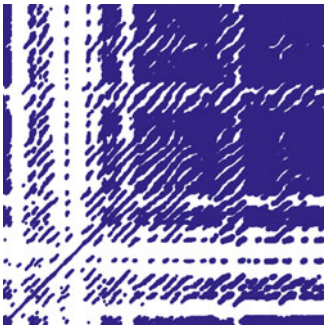

Abstract Otoacoustic emissions are sounds generated inside the inner ear. Recurrence Quantification Analysis (RQA) has proven to be particularly suited for studying such signals, being able to evidence their essential dynamical characteristics. In this chapter the fundamental features of the auditory system will be briefly reviewed, then the results obtained in the literature, and linked to the application of RQA to otoacoustic emissions, will be reported and discussed.

8.1 Introduction

In this chapter the potentialities of the RQA technique are described with reference to otoacoustic signals, which are signals recorded in the ear canal and which are used clinically for the diagnosis of hearing losses. RQA is extremely fit to study non-stationary signals, as otoacoustic signals, and represents a valid alternative to wavelet analysis. In fact, the embedding procedure allows to expand the otoacoustic mono-dimensional signal into a multidimensional space, thus letting the identification of subtle peculiarities of the sampled series that in turn are described by few

G. Zimatore (✉)
CNR-IDASC – Institute of Acoustics and Sensor "O.M. Corbino", Rome, Italy
e-mail: giovanna.zimatore@uniroma1.it

M. Cavagnaro
DIET – Sapienza University of Rome, Rome, Italy
e-mail: cavagnaro@diet.uniroma1.it

C.L. Webber, Jr. and N. Marwan (eds.), *Recurrence Quantification Analysis*,
Understanding Complex Systems, DOI 10.1007/978-3-319-07155-8_8,

global parameters. In this way a synthetic description of the characteristics of very complex signals is allowed.

RQA has proven to be able to assess the fine structure of otoacoustic signals without any a priori hypothesis (i.e. stationarity) and any data manipulation; moreover it has proven to be independent from differences in signal amplitude.

The chapter is introduced with a brief description of ear morphology and physiology. This description is not intended to be exhaustive but it allows understanding the origin of the different hearing losses and the existence of sounds generated by the inner structures of the ear, named otoacoustic emissions. The hearing losses as well as the ear-generated sounds are reviewed in the successive paragraphs. Then, the different instrumentation used in clinical settings to diagnose hearing losses is briefly depicted. Successively, three paragraphs are devoted to the possible applications of RQA to study the different features of otoacoustic emissions, reporting promising results of research studies. It is the Authors' hope that at the end of the chapter the reader will be able to understand the fundamental characteristics of otoacoustic emissions, and to appreciate the tremendous potentialities that the RQA technique has on evaluating such characteristics.

8.2 Ear Morphology and Physiology

The auditory system can be subdivided into a peripheral and a central auditory system. The peripheral system converts the sound energy, represented by condensations and rarefactions of air molecules, into neural codes that are interpreted by the central auditory system as specific sound tokens [1].

The peripheral auditory system is in turn divided into the external ear, made by the auricle and the external ear canal, the middle ear, which stands between the tympanic membrane and the oval window, and the inner ear corresponding to the cochlea and semicircular canals of the vestibular system (Fig. 8.1).

The external ear collects the sound waves and converts them into mechanical motion at the eardrum. This motion is transferred through the middle ear ossicles (malleus, incus, stapes) up to the oval window, where it is converted into a pressure wave and transferred to the inner ear organs (Fig. 8.2). Here, it is finally analyzed and converted into neural codes that are carried by the auditory nerve to the central auditory system (acoustic cortex).

The cochlea is a shell shaped organ, filled with incompressible fluids. In the human ear it is made by 2 and 3/4 turns for a total unrolled length of about 35 mm. The cochlea is divided into three canals: the scala vestibuli and scala tympani, which are filled with the perilymph fluid and linked through the helicotrema at the cochlea apex (Fig. 8.2), and the scala media, which is filled with endolymph and it is isolated from the other two scales by the basilar membrane and the Reissner's membrane (Fig. 8.3).

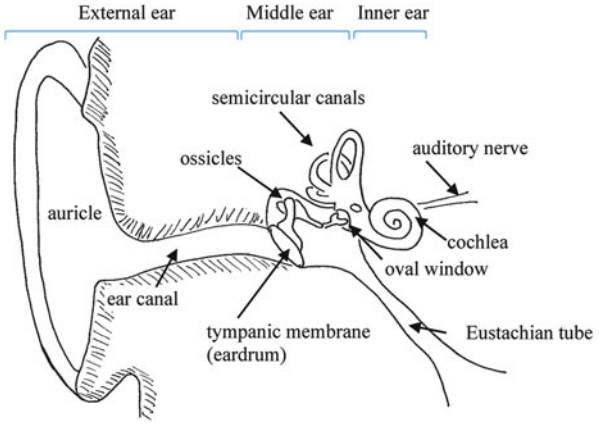

Fig. 8.1 Schematic view of the peripheral auditory system showing the ear canal, tympanic membrane, middle ear ossicles, and the inner ear made by the cochlea and semicircular canals of the vestibular system

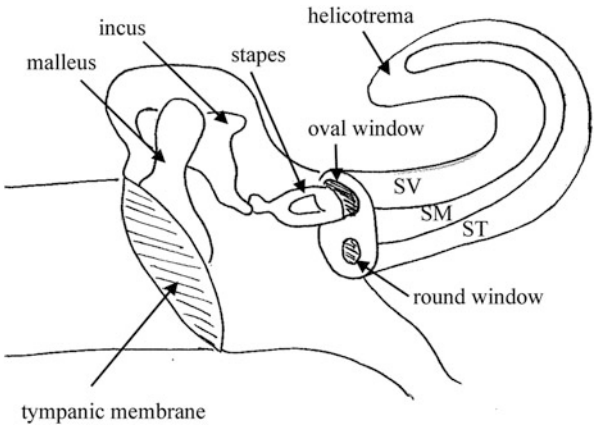

Fig. 8.2 Schematic view of a longitudinal section of uncoiled cochlea showing the oval window, and the scala vestibuli (*SV*), scala media (*SM*) and scala tympani (*ST*) within the cochlea

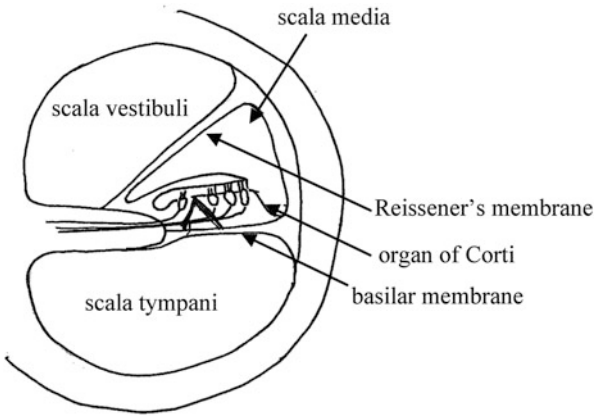

Fig. 8.3 Schematic view of a cross section of the cochlea showing the scala vestibuli (*SV*), scala media (*SM*) and scala tympani (*ST*). The organ of Corti is also evidenced

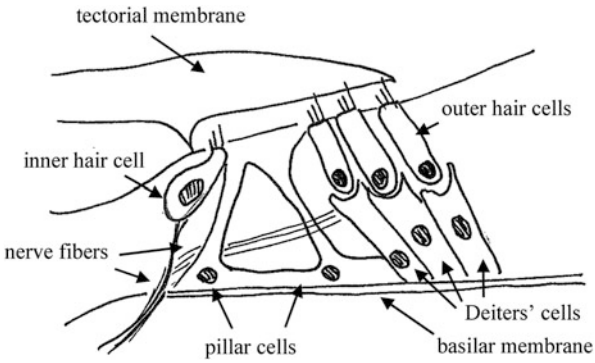

Fig. 8.4 Schematic view of a section of the organ of Corti. The pillar cells, Deiters' cells, outer and inner hair cells are shown

On the basilar membrane stands the organ of Corti, which is responsible for the transduction of the pressure waves into neural signals. The Corti's organ extends between the basilar and the tectorial membrane within the scala media (Fig. 8.4). It is made by a series of structures that repeat themselves all along the cochlea (in the human ear their number is about 3,500).

These structures are constituted by several types of cells each with a specific role for the sound transduction (Fig. 8.4): the pillar cells which contribute to the mechanical stability of the organ of Corti and shape a tunnel where nerve fibers run; the Deiters' cells which form the base of the Outer Hair Cells (OHC) and help amplifying or dumping the incoming pressure wave; the OHC, which are equipped with cilia terminating into the tectorial membrane and are organized in three lines, and finally the Inner Hair Cells (IHC), one every three OHC, which have cilia not terminating into the tectorial membrane.

Fluid and tissue displacements travel from the oval window all along the cochlea from the base to the apex. Pressure relief is provided for the incompressible fluids of the inner ear by the round window membrane (Fig. 8.2). Under the action of the fluid pressure, the basilar membrane and the OHC, which are in-built on it, oscillate. Due to these oscillations the OHC cilia bend, provoking the opening of ion channels and the depolarization of the cells that, as a consequence, shrink.

The OHC contraction is selectively amplified by the Deiters' cells. Moreover, the OHC organization on the basilar membrane is such that, when a pressure wave stimulates the OHCs, the stimulus is amplified only by the cells located in a particular position of the basilar membrane, corresponding to the frequency of the incoming sound. This organization is defined as tonotopic and helps de-codifying the different frequencies composing a sound: higher frequencies are detected close to the base of the cochlea, while lower frequencies travel longer along it. The OHC action causes the movement of the tectorial membrane, which drags along the movement of the IHC cilia. Since IHCs are contacted by nerve fibres that link the organ of Corti with the cochlear nuclei in the brainstem, the movement of IHC cilia finally stimulates the auditory nerve.

According to the previous description, the position of the IHCs that stimulate the nerve fibers carries on the information on the frequency of the incoming stimulus. On the contrary, the number of nerve fibers activated is proportional to the intensity of the acoustic stimuli. In this way the acoustic cortex can elaborate real time information about frequency and intensity of incoming sounds.

8.3 Otoacoustic Emissions (OAE)

OAEs are low-level sounds generated in the inner ear and measurable in the external auditory canal [2]. They can be recorded in a normal ear when the auditory periphery is solicited by an external acoustic stimulus, such as a transient sound (Transient evoked OAE, TEOAE) or two pure tones (Distortion Product OAE, DPOAEs), and even in the absence of stimulation (Spontaneous OAE, SOAE) [3].

The actual origin of OAE is still unclear. Nowadays, their generation has been explained as the combination of two mechanisms: a linear reflection of the incident traveling wave within the inner ear, due to irregular discontinuities of the basilar membrane [4, 5], and a nonlinear distortion process based on the active contractile mechanisms of the OHC in the Corti's organ [6–9]. Even if a general consensus on the presence of the two mechanisms is lacking, it is generally agreed that OHC active processes are fundamental in OAE generation.

OAE represent an objective, non-invasive test that can assess with great accuracy OHC activity, as demonstrated by experimental and clinical studies [10–12]. Their evaluation does not need the collaboration of the patient, and they show a great reproducibility and stability in time. Accordingly, OAE have been increasingly used in clinical applications, e.g. for the assessment of ear functionality in newborn babies. Moreover, they have been used to monitor the cochlear effects of exogenous factors, such as ototoxic drugs, solvents, and high-level sound exposure [13, 14]. Recently TEOAE were used to study tinnitus subjects with normal hearing to assess whether a minor cochlear or efferent dysfunction might play a role in tinnitus [15].

8.4 Hearing Losses

The lowest sound that an average person is able to hear (hearing threshold) has an amplitude of about 20 decibel. The decibel (dB, or dB HL) is a logarithmic scale normalized to the maximum value. A person with a hearing threshold higher than that of an average person is said to have hearing losses. At present, about 360 million people worldwide have disabling hearing losses [16].

Hearing losses can be classified as conductive, sensory-neural, and retrocochlear or central [17]. In the first case the damage responsible for the hearing loss is located in the external or in the middle ear, so that the sound path is interrupted; in the second case the damage is located in the inner ear, while in central hearing loss the damage is located along the pathway from the cochlea to the cortex.

Several external as well as internal agents can induce hearing loss, with different consequences both on the ear physiology and functionality. Conductive hearing losses can be due to trauma, that can damage the tympanic membrane or disrupt the ossicle chain, or by otosclerosis. Sensory-neural hearing losses are linked to the death of OHC. This can be the result of ageing, of exposure to drug or to high level sounds or noise.

In the following, the age-related hearing losses and those associated to noise exposure will be briefly reviewed.

8.4.1 Age-Related Hearing Loss (ARHL)

Age Related Hearing Loss (ARHL), also referred to as presbycusis, is the progressive deterioration of hearing ability that occurs with normal aging and it is one of the most chronic conditions in elderly people [18]. ARHL affects 23 % of the population between 65 and 75 years of age, and 40 % of the population older than 75 years in the USA. In Europe, it affects 2.3 % of the population between 40 and 50 years of age, and over than 30 % of the population above 70 years [19]. Presbycusis is common in industrialized societies and is less pronounced in other societies. This discrepancy has been attributed to many factors including genetics, diet, and socioeconomic and environmental factors.

The pioneering work in the investigation of age-related hearing loss (ARHL) was by Schuknecht et al. [20, 21], which defined four types of ARHL according to the origin of the lesion: sensory, strial, conductive and neural. Sensory loss is characterized by the death of the outer hair cells (OHCs) in the Corti's organ, usually beginning with the OHC located at the cochlea's base where the higher frequencies of the sounds are detected, and then progressing toward the apex where the lower frequencies are detected. Strial loss, also referred to as metabolic loss, is linked to the atrophy of the capillary and blood vessels, which help maintaining the metabolic processes of the cochlea. Strial loss is a process that involves the whole cochlea. Conductive loss is due to the loss of motility of the basilar membrane due to its thickening and stiffening, while neural loss corresponds to the dead of nerve cells. Several studies have identified a complex interaction between intrinsic (genetic) and extrinsic (environmental) factors at the basis of ARHL [22–25], so that nowadays there is a general consensus on considering this inevitable deterioration in hearing ability a multifactorial process [23, 24, 26, 27].

8.4.2 Noise Induced Hearing Loss (NIHL)

Noise Induced Hearing Loss (NIHL) is a sensory-neural hearing loss with great public health relevance. Every year, approximately 30 million people in the United States and 30 million people in Europe are exposed to occupational noise [19, 28, 29].

Prolonged exposure to intense noise can induce a transitory fatigue of the organ of Corti, which in turn leads to a transitory rise of the hearing threshold levels, i.e. a rise of the intensity of the minimum audible incoming sound, or can induce a permanent damage with particular reference to the higher frequencies.

Depending on the intensity of the noise, multiple anatomical changes can be found in the inner ear after the acoustic trauma, ranging from distorted stereocilia of inner and outer hair cells, to a complete destruction of OHCs followed by IHCs death and rupture of intracochlear membranes. Death of hair cells may also result in a partial degeneration of spiral ganglion neurons [30]. Many studies have shown that the generation of reactive oxygen species (ROS) and free radicals is involved in the cascade of cochlear events induced by the acoustic trauma [31]. A synaptic repair mechanism can occur within the first few days post-exposure, partially helping in the recovery of acute hearing loss (temporary threshold shifts, TTS) [32]. However, whereas most epithelial tissues present a high turnover rate and tend to regenerate after a traumatic lesion, the mammalian cochlea does not have regenerative properties leading to irreversible hearing loss. Different approaches have been used to prevent noise induced hearing loss such as antioxidant drugs [14, 33–36].

8.5 Clinical Practice

Tests performed to discern hearing losses include: tympanometry, electrocochleography, evoked potential, pure tone audiometry, and the ILO test. In particular, pure tone audiometry and the ILO test are those more widely used in the clinical practice; they will be briefly reviewed in the following.

8.5.1 Pure Tone Audiometry

The pure tone audiometry (PTA) is the more widespread method used in the assessment of hearing. It consists in the evaluation of the hearing threshold at different frequencies: at each considered frequency, pure tones are presented into the aural canal with decreasing intensities until the patient is no longer able to hear them. Although the human auditory range is from 20 to 20,000 Hz, PTA covers in a strict sense the speech spectrum: 250, 500, 1,000, 2,000, 3,000, 4,000, 6,000 and

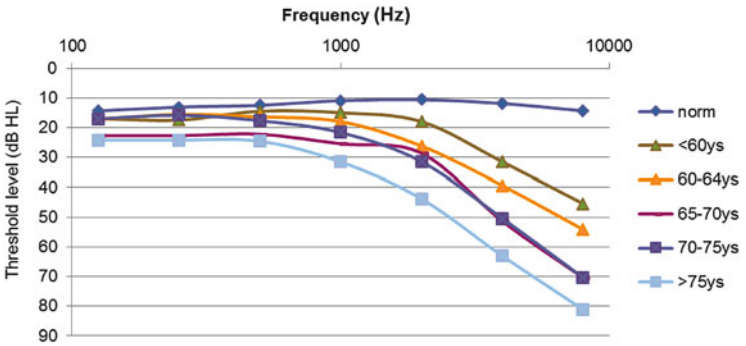

Fig. 8.5 Audiogram with the mean threshold values for five age-groups

8,000 Hz. The PTA output is a graphical representation of the obtained thresholds (audiogram) with the frequency in hertz (Hz) on the horizontal axis and the hearing level (HL) measured in dB on the vertical axis. On the PTA graphs the hearing thresholds are reported in an inverted way: the higher the threshold, the lower the position within the vertical scale. Starting from a normal threshold from 0 to 20 dB at all frequencies, a 6 dB increase in the hearing threshold represents a doubling of sound pressure level. Accordingly, hearing loss is classified according to how far the marks go down on the audiogram, and at what frequencies that occurs. PTA is a subjective test, which needs the active cooperation of the patient. As a consequence it can neither be performed on young babies nor on mentally retarded or elderly people with brain disorders.

Figure 8.5 shows the characteristic differences in threshold levels due to the increasing age. From the figure it can be noted a progressive loss of hearing sensitivity at higher frequencies. However, as noted before, ARHL is a multifactorial process so that it could be the result of a combination of different loss types and the estimate of the dominant contribution to the loss cannot be made on the basis of an audiogram alone.

When the hearing loss is due to noise exposure, the audiogram shape shows a characteristic notch at the frequency of 4 kHz. As an example, Fig. 8.6 shows the audiogram obtained from normal ears (grey line), and NIHL ears (black line).

The peculiar shape of NIHL audiogram is due to the fact that the human ear is particularly sensible at this frequency, so that the OHC located at the tonotopic position of 4 kHz are the first to die when the ear collects sounds too high. Some authors identified in 6 kHz another frequency sensible to sound damage [37, 38].

8.5.2 ILO Test

The ILO test is performed through the Otodynamic Analyzer (ILO92, Otodynamics Ltd., Hatfield, UK) developed by Kemp after his discovering of OAE [2]. The

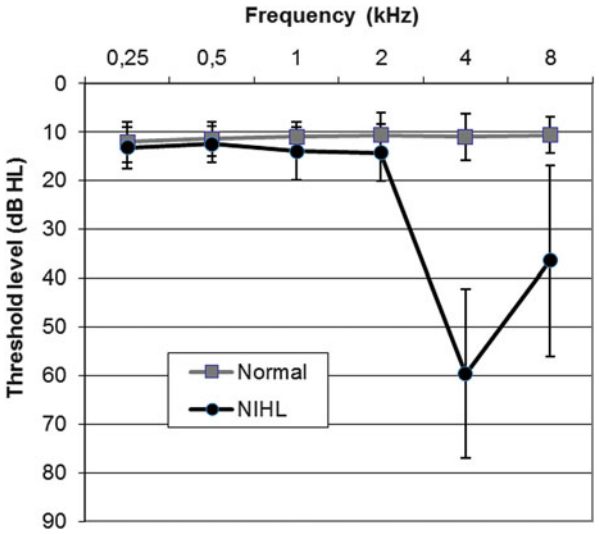

Fig. 8.6 Mean pure-tone hearing thresholds for normal ears (*square symbols* and *grey line*) and NIHL (*circle* and *black line*). *Bars* represent the standard deviation from the mean. Reproduced with permission [74]

ILO test is based on the measurements of OAEs through commercial devices (the ILO88 or ILO92; Otodynamics Ltd., Hatfield, UK) and on the evaluation of the reproducibility and signal to noise ratio of the measured waveforms. In the clinical practice protocols based on TEOAEs are widely used for identifying hearing losses [3, 39–41] and, as in DPOAEs, may provide an early indication of cochlear damage before evidence of NIHL appears in pure-tone audiometry.

The TEOAE signal is recorded at the ear canal in response to a stimulus. It includes a passive ringing of the speaker, ear canal, and middle ear, substantially linear with the incident stimulus and arriving with short latencies. This ringing is followed by a smaller, long-latency and long-duration oscillation constituting the non-linear TEOAE [42]. Figure 8.7 shows a TEOAE waveform recorded from a normal ear, after removing the first 2.5 ms to rule out the initial ringing. According to the tonotopic organization of the OHCs within the cochlea, the TEOAE signal presents a characteristic latency of the different frequencies composing the signal, with the higher frequencies coming first, followed by the lower frequencies (Fig. 8.7).

To better discriminate the TEAOE signal with respect to the initial ringing as well as to the background noise, a non-linear estimation method has been developed [43]. In this method the stimulus is made of a train of three rectangular pulses of equal amplitude and polarity (75–85 dB sound pressure level—SPL) lasting 80 μs followed by a fourth pulse three times higher than the previous ones and with inverted polarity [43]. The clinical signal is obtained sending 520 stimuli trains, for a total of 2,080 clicks, recording the obtained TEOAE in two different buffers, and evaluating the average signal in each buffer. Then the correlation between the two averaged waveforms is evaluated (Pearson correlation coefficient × 100). According to the clinical settings, when the whole waveform reproducibility (REPRO or

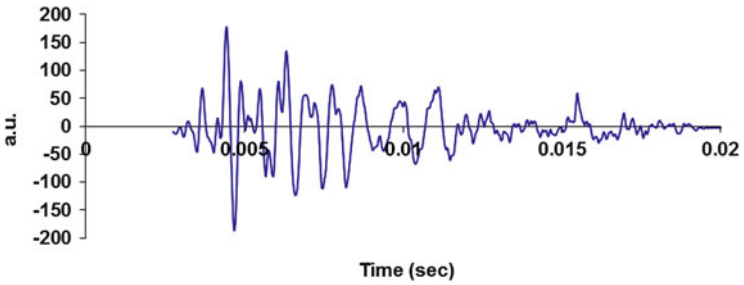

Fig. 8.7 TEOAE signal recorded from a normal ear

WWR) value is higher than 70 and the SNR (Signal to Noise Ratio) is higher than 3 dB, the signal is considered as physiological (ILO Test is Passed), whereas a WWR value lower than 70 indicates the presence of a possible hearing malfunction (ILO Test is Failed) [44].

OAEs tests are non-invasive and do not require co-operation from the patient, as does audiometry instead; still, 30 years after their discovery, clinical applications of OAEs are largely limited to qualitative pass/fail testing [2, 10, 45].

Researches have suggested that OAEs may provide early indication of cochlear damage before evidence for hearing loss appears in pure-tone audiometry [46, 47].

In particular, Lucertini et al. [48] compared TEOAE variables with pure tone audiograms, showing that the firsts could discriminate between non-exposed normal subjects and subjects with unilateral noise-induced hearing loss. Accordingly, OAE can be used to monitor subjects at risk of hearing impairment, as workers in noisy environment or patients receiving lifesaving ototoxic drugs. Moreover, since OAE are generated in the inner ear and propagate toward the middle to the external ear, they can be used to discriminate among different causes of hearing loss [42]. However, the validity of TEOAE measurements is hampered by their subject-dependent variations [45].

8.6 RQA to Study the Characteristics of Otoacoustic Emissions

In this section results obtained studying the TEOAE signal by way of RQA will be reviewed in order to emphasize the great potentiality both of the TEOAE signal and of the RQA analysis for improving the knowledge of the human ear physiology and building the basis for developing new methods of diagnosis. RQA is particularly suited for studying OAE being not limited by specific requirements on the studied signal, like stationary or length of data series, and being able to quantitatively evidence the amount of deterministic structure of a signal [49, 50].

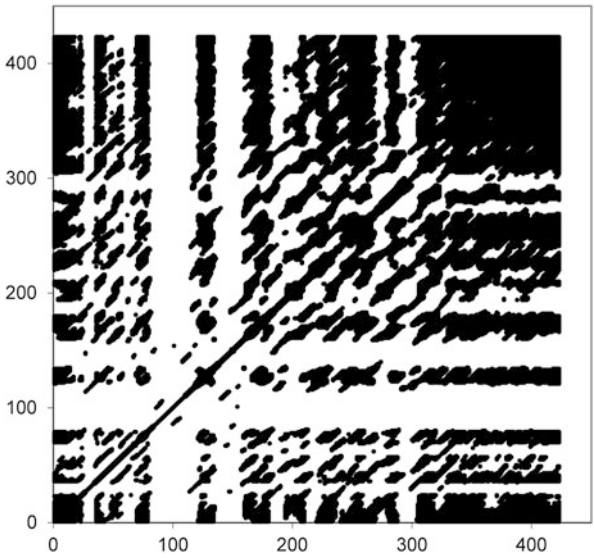

Fig. 8.8 Recurrence plot of a typical TEOAE recorded in a normal ear (DET = 86.01)

Figure 8.8 shows the Recurrence plot of a typical TEOAE recorded in a normal ear. Three RQA descriptors proved to be the most suitable in the study of TEOAE signals through RQA [51]: Percent Recurrence (REC), which represents the fraction of the recurrence plot occupied by recurrent points, measuring the amount of recurrent (both periodic and auto-similar) behavior of the signal; Percent Determinism (DET), that is the fraction of recurrent points aligned parallel to the main diagonal (deterministic lines) and indicates the degree of deterministic structures of the signal; Entropy (ENT), which is a Shannon entropy estimated over the distribution of the length of deterministic lines, and it is linked to the richness of deterministic structure. The RQA descriptors REC, DET, ENT were calculated with the following choice of working parameters: time course of the original signal described by 512 points; delay in the embedding procedure (lag) equal to 1; 10 columns included in the embedding matrix (embedding dimension); cut-off distance (radius) equal to 15 [51]. The ability of the RQA technique to represent the main features of TEOAE signals was evidenced in a study which compared the two recurrence plots (not shown) obtained from a TEOAE signal as well as from its shuffled version [51]. The comparison showed that while the TEOAE signal exhibited a rich deterministic structure, this was no longer present after shuffling. Moreover, all three RQA descriptors REC, DET, and ENT evaluated on the TEOAE signal showed a correlation with the ILO REPRO value. In particular, studying TEOAE signals as a function of the intensity of the stimulus, it was found that the DET descriptor changed, starting from a sub-threshold state, going through a phase of linear increase with the stimulus, and finally coming to a saturation phase in which it did not change with the intensity of the stimulus any more. These

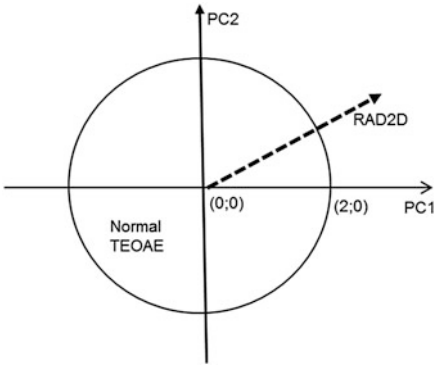

Fig. 8.9 NA circle in the PC1/PC2 plane

changes of the DET value for different stimulus intensities correspond to a higher organization of the TEOAE signal with the increasing stimulus [52].

The three RQA descriptors were analyzed through Principal Component Analysis (PCA), a statistical technique which projects a multidimensional data set into a space of orthogonal axes, called principal components (PC) [53]. PC are selected, one after the other (PC1, PC2, etc.), on the basis of the maximal variance explained in the space of the original variables. The presence of correlations between the original variables allows reducing the data set dimension in the new space without noticeable loss of information. Zimatore et al. [51, 52] showed that, choosing a set of at least 70 TEOAE signals as a reference (training set) for the RQA–PCA analysis, the first two principal components (PC1, PC2) can explain more than 90 % of the observed variability. Moreover, since PC1 and PC2 have, by construction, zero mean and standard deviation equal to 1.96 % of real signals, if taken from a homogeneous population, should fall within a circle centered in the origin of the PC1/PC2 plane with radius equal to 2 (NA circle), thus allowing for a straightforward test of 'normality' [51]. Figure 8.9 shows the PC1/PC2 plane with the NA circle evidenced.

The RQA/PCA analysis was applied to the study of TEOAE signals to find out subject-dependent characteristics, which could be used to evidence TEOAE features, and subsequently correlated to changes in ear physiology. The first observation that could be performed was that representing on the PC plane different TEOAE signals measured from different subjects, signals recorded from different ears located in different positions of the PC plane, while signals recorded from the same ear of the same subject located close each other [51]. However, it was noted that if the stimulus used to record the TEOAE was of medium intensity, the clustering of signals coming from the same ear was not present. On the other hand, the clustering was present when high-level stimulus intensities were considered [52].

Since TEOAE can be recorded without the need of an active cooperation from the subject, they are extensively used in neonatal screening of the ear functionality. It is well known that the neonatal TEOAE responses are characterized by a large

intra-subject variability (up to 6 year of age) [54–56], by larger signal amplitudes with respect to the adult ones [57, 10] and by a wider and more uniform spectrum, sometimes shifted toward the higher frequencies [58]. Comparing the RQA/PCA descriptors obtained by TEOAE recorded in newborn babies and in adults, DET values in the neonatal group were lower than those from the adult subjects, indicating a minor presence of determinism in the neonatal signals [59]. Moreover, both the inter-subject variability and the intra-subject variability were larger in newborns than in adults, showing a weakness of the REPRO value of the ILO test in the evaluation of newborn acoustic performances. Finally, the ratio of inter-subject to intra-subject variability had similar values in the two groups, pointing to the presence of the same amount of individual features, i.e. the individual characteristics of the TEOAE signal are present since the very beginning of life [59]. However, it is interesting to note that no correlations were obtained between signals from the two ears of the same subject. This implies that origin of TEOAE individual features should be searched on a micro-scale level, e.g. as a different distribution of OHCs, which could be different in the two ears even for newborns.

8.7 RQA and Models of the Ear to Study the Origin of Otoacoustic Emissions

Many researchers are interested in modeling the dynamic behavior of the cochlea or in physically interpreting the results of cochlear measurements. The objectives are to produce tools that can be used to predict the response of the cochlea to various inputs thus helping in developing devices to overcome hearing losses.

Several models of the ear have been developed with the aim of studying the ear functionality, with reference to speech, hearing, and OAE. These models can be broadly divided into two categories: functional and physical models [60, 61]. Functional models, such as the gammatone [59, 62] or the electronic cochlea [63], aim at reproducing a specific behavior of the ear, as e.g. the general shape of TEOAE, without looking for a correspondence between model elements and anatomical structures. On the contrary, physical models are based on a strict correspondence between the two. Within the latter models, those based on the electroacoustic analogy substitute acoustic quantities, as sound pressure and volume velocity, with electric quantities like voltage and current, respectively [64].

In the gammatone model it is supposed that the inner ear behaves as a bank of narrowband filters, each centered on a specific frequency (f_c). In the time domain, the impulse response of a filter is given by:

$$\gamma(t) = at^3 e^{-\beta\omega_c t} \cos(\omega_c t) \tag{8.1}$$

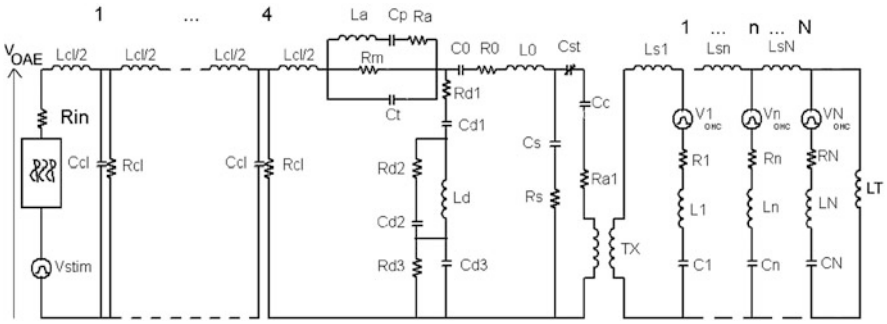

Fig. 8.10 Ear model based on the electro-acoustic analogy. Reproduced with permission [70]

where t is the time, $\omega_c = 2\pi f_c$ is the angular frequency, $a = (\omega_c)^{3.5}$ is an amplitude factor used to obtain a gammatone power independent from the frequency, and β represents the signal dumping [62].

In this model, it is supposed that the TEOAE signal is the sum of the impulse responses of each filter. In effect, if a set of five gammatones is used, centered at the frequencies of 1.0, 1.5, 2.2, 3.3, and 5.0 kHz and with a dumping factor β of 0.11 [62], a TEOAE waveform with a shape close to the real one is obtained [59]. However, if the thus obtained TEOAE waveform is studied with a single value decomposition (SVD) analysis, which aims at evaluating the number of independent modes (eigenvalues) excited in a system from the percentage of variance explained by each eigenvalue, it is found that the gammatone model generates a TEOAE signal more complex than the real one. In fact, more modes were needed to explain the same percentage of variability than the real signal, probably due to the lack of coupling between the different gammatone filters [59].

More interesting results have been obtained by using the model of the ear developed by Giguère and Woodland [65, 66], and the RQA/PCA technique [67]. The Giguère and Woodland [65, 66] model is based on the electroacoustic analogy, which, as already cited, represents the sound pressure with the electric voltage and the volume velocity with electric current. In this model, shown in Fig. 8.10, the outer ear is represented with a cascade of four T-sections, corresponding to the segmented form of an uniform transmission line [68], and the middle ear is modeled as a complex electrical network based on its functional anatomy [69]. An ideal transformer connects the middle ear to the cochlea, to represent the acoustic transformer ratio between the eardrum and the oval window [65]. The cochlea is modeled as an active non-uniform and non-linear transmission line, divided into several sections (named partitions) from its base to the apex.

Each partition consists of a series inductor, a shunt resonant circuit (composed of a resistor, an inductor, and a capacitor), and a non-linear voltage source. In the electro-acoustic analogy, the series inductors represent the acoustic mass of the cochlear fluids; the resistors, inductors and capacitors forming the shunt resonant circuits represent the acoustic resistance, mass and stiffness of the basilar

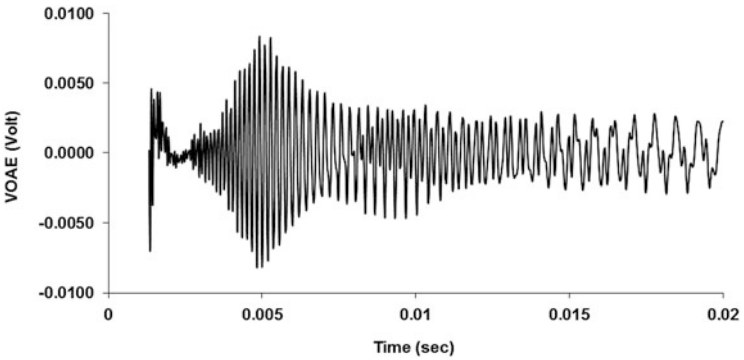

Fig. 8.11 TEOAE simulated signal

membrane, respectively, and the non-linear voltage sources represent the OHC active processes. Finally, an inductor models the helicotrema (L_T). Spontaneous OAE can be simulated inserting random noise sources into the cochlea partitions. To simulate TEOAE, the ear model is fed with a voltage source modeling the clinical set-up. The input voltage is a rectangular pulse 80 μs wide, whose amplitude corresponds to a stimulus of 80 dB SPL. The loudspeaker influence on the input signal is considered by inserting a band-pass filter ($f_{LOW} = 6$ kHz, $f_{HIGH} = 20$ kHz, ripple 3 dB, stop-band 5 dB) in series with the input voltage source (Fig. 8.10).

The Giguère and Woodland's model was adapted to be solved through the commercial software PSpice® [67] by using the parameter values proposed in [65]. In particular, the cochlea has been initially modeled by using 128 sections according to what done by Giguère and Woodland [65].

The TEOAE simulated signal is reported in Fig. 8.11. From the figure it can be noted that the simulated signal is close to the signal recorded from a normoacoustic subject [67]. In particular, the simulated signal, after removing the firsts 2.5 ms, to eliminate the initial ringing, shows an oscillating behavior with time lasting up to 20 ms after the initial external excitation, and the typical latency-frequency TEOAE behavior, that is to say the higher frequencies have a shorter latency, and the lower frequencies have a longer one.

Figure 8.12 shows the latency of the simulated TEOAE signal compared with the latency of the real signal. The data are obtained evaluating, through a wavelet analysis, the time needed for each frequency that compose the TEOAE signal to cover the round trip from the oval window to the corresponding resonant partition and back. From the figure a good agreement can be obtained between the different curves. However, if the slope of the latency–frequency curve is evaluated, a value of -0.8 is obtained for the simulated signal, higher than that usually obtained from normoacoustic subjects (about -0.48), but in agreement with the outputs of models which use the transmission line formalism to represent the cochlea [71]. In fact, in [72] it is noted that an inverse proportionality relationship between latency and frequency (i.e. a slope of -1) is inherent to scale invariant cochlear models, which

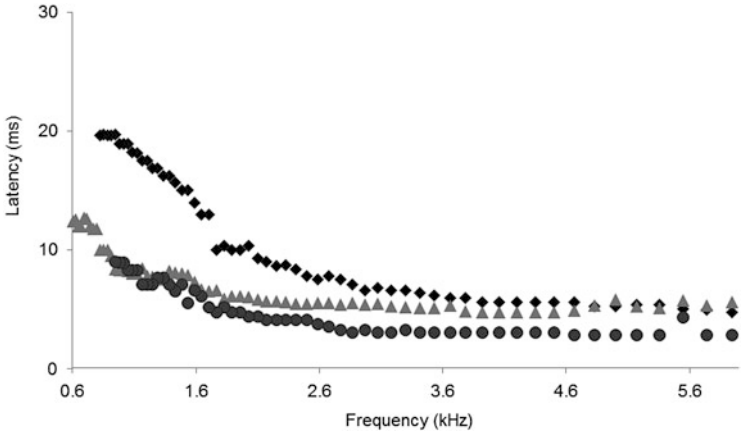

Fig. 8.12 Latency of TEOAE signals as a function of frequency. *Grey triangles*: measured TEOAE, *black diamonds*: TEOAE simulated using 128 partitions to model the cochlea; *black circles*: TEOAE simulated using 64 partitions to model the cochlea

are, in the transmission line formalism, the models with a constant quality factor (Q) in all the cochlea sections, as the electronic model [65].

To ameliorate the latency–frequency behavior of the simulated signal without changing the ear model, the characteristics of the transmission line which models the cochlea can be exploited. In fact, each section modeling the cochlea induces a time delay on the traveling signal, as a function of both position and frequency. Consequently, lowering the number of cochlear sections could reduce the time delay in the simulated signal; moreover, since the higher frequencies travel along the transmission line for a lower number of sections with respect to the lower frequencies (each frequency travels up to its tonotopic site, where the wave is reflected back on the line), this time delay reduction should be more pronounced for the lower frequency components of the signal. This, in turn, should lower the latency-frequency slope of the simulated signal. This strategy, of decreasing the number of cochlear sections used in the model, has to be intended as a best fitting procedure, justified by the typical redundancy of biology systems, void of any one-to-one mapping of the biological reality.

Following these considerations, a circuit with 64 partitions representing the cochlea has been developed, and the obtained signal has been compared with a real signal and with the one obtained from the 128-partitions model. While the time waveform of the signal is as close to the real one as the 128-partition model signal, the slope of the latency–frequency curve (see Fig. 8.12) for the 64-partitions signal was evaluated as equal to −0.60, i.e. closer to the real one. Other characteristics have been evaluated as e.g. the basilar membrane volume velocity, reflections from the different sections modeling the cochlea, all showing a better agreement of the 64-partitions model to the real signal than the 128-partitions model.

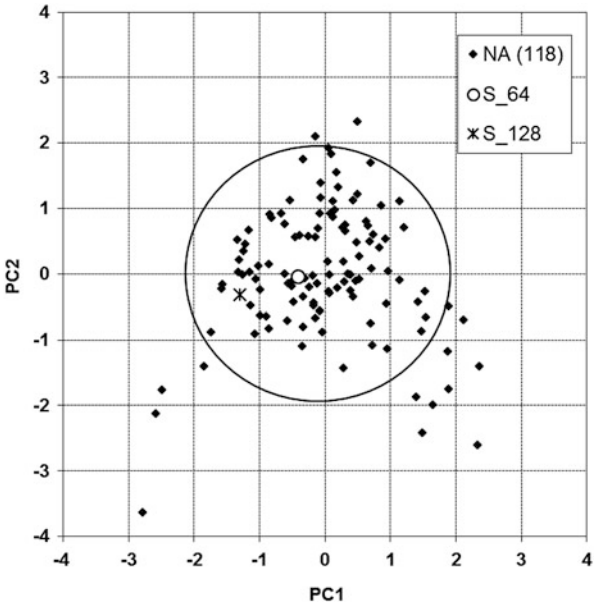

Fig. 8.13 TEOAE signals in the PC1/PC2 plane after RQA/PCA analysis. *NA*: normoacoustic ear, S_64: simulated TEOAE with the 64-partitions model, S_128: simulated TEOAE with the 128-partitions model

Coming to the RQA/PCA technique, it was found that the simulated signal falls well within the NA circle in the PC1–PC2 plane. Figure 8.13 shows the NA circle obtained from 104 TEOAE signals recorded from normoacoustic ears. In the figure the diamonds represent the 104 signals, confirming that more than 96 % of real signal, if taken from a homogeneous population, fall within the NA circle. Moreover, in the figure the signal obtained from the 128-partitions model (square), and that obtained from the 64-partition model (circle) are also reported. From the figure it can be obtained once again that the 64-partitions model gives a simulated signal close to a real one, falling well within the NA circle.

The electric circuit modeling the ear can be used to study the influence of individual variability on the TEOAE signal. To this end, some middle ear elements were properly changed according to the experimental findings of Avan et al. [11], as reported in Table 8.1. In the table, C_{st} represents a stapes capacitor (see Fig. 8.10). When C_{st} has a large value, its impedance is small, corresponding to small tension in the stapedius muscle (C_{st} equal to infinity corresponds to no stiffness in the resting condition); conversely, when C_{st} is small, its impedance is large, corresponding to muscle high tension. C_{st} was equal to infinity in the model proposed by Giguère and Woodland [65], so that this condition is considered as the reference one. C_0 represents changes in the tympanic membrane stiffness, to account for changes in the middle ear pressure, while L_0 represents changes in the tympanic membrane mass, to simulate an additive mass. All the parameters' values reported in the table correspond to physiologic conditions [11].

Figure 8.14 reports the simulated TEOAE signals in the PC1/PC2 plane. As can be noted from the figure, the position of the points in the PC1/PC2 plane

Table 8.1 Values of the middle ear parameters used to simulate individual variability [11]

Set	C_{st} (μF)	C_0 (μF)	L_0 (mH)
Ref	∞	1.40	40
1	0.25	1.40	40
2	0.25	0.700	40
3	0.25	0.233	40
4	0.25	1.40	80
5	0.25	1.40	160

The first row reports the starting values (reference set)

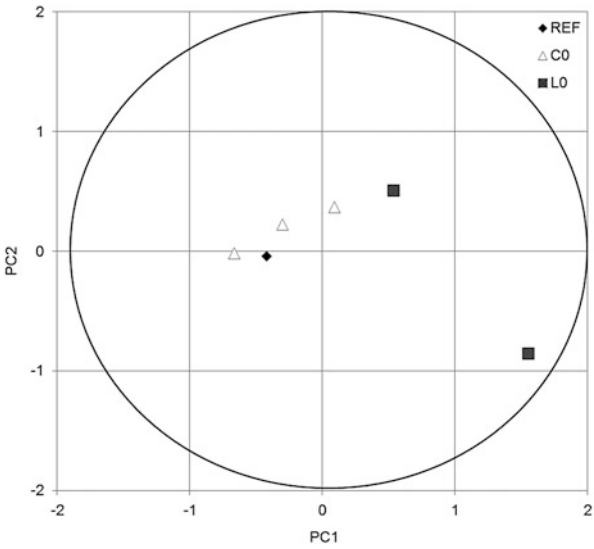

Fig. 8.14 Simulated TEOAE signals in the PC1/PC2 plane after RQA/PCA analysis. The *different symbols* represent different values of some parameters of the middle ear (see text)

changes when the value of a parameter of the middle ear section is changed, but the signal remains within the NA circle. As a consequence, it could be supposed that differences in the middle ear anatomy contribute to individual variability of TEOAE signals.

8.8 RQA in the Diagnosis of Hearing Losses

The complexity and fragility of the inner ear makes it extremely susceptible to damage. Research has shown that the most common cause of deafness is the loss of hair cells and not the loss of auditory neurons. In fact, OHCs represent the most sensitive and consequently the most vulnerable part of the ear.

Being the TEOAEs generated by OHC and transmitted through the middle ear and the ear canal, they reflect functions of outer hair cells (OHCs), and in some extent of the middle ear and ear canal also. However, if the damage is of limited

entity, it may not be detected by looking at the general characteristics of TEOAE. On the contrary, by studying the properties of TEOAEs through RQA, it is possible to discriminate different hearing losses and even to evidence inner ear damages before they can be evidenced by standard audiology tests. In the following lines the application of the RQA/PCA technique for the detection and discrimination of different hearing losses will be shown.

8.8.1 RQA Applied to the Study of CHL and SHL

In clinical applications the main problem of OAE consists in the large observed inter-subject variability, resulting in a different relationship between reproducibility and audiometric thresholds for different ears. In fact, it was found that the same audiometric threshold was associated with different REPRO values [73]. Moreover, subject-dependent variations in middle-ear transmittance and reflectance influence OAEs, and should be controlled [45]. The validity of OAE measurements can be increased by reducing their variance. This can be easily performed through the RQA technique. In Zimatore et al. [52], RQA was applied to TEOAE signals recorded from CHL and SHL ears at four intensities of the incoming stimulus (50, 65, 70, and 80 dB). In that work it was shown that the DET value was significantly different between the two groups of pathological signals, as well as between each of the two pathologies and the control group. This result points to the suitability of RQA in discriminating among the different pathologies. Figure 8.15 shows the TEOAE signals recorded from normal, CHL and SHL ears projected in the PC1/PC2 plane after the RQA/PCA analysis. From the figure it can be noted that while CHL signals move towards the negative axes, going away from the plane center and from the NA circle, SHL signals tend to superimpose to the normal ones, indicating still the presence of TEOAE essential features. Nevertheless, as said, the DET variable was able to discriminate among the three different groups [52].

8.8.2 RQA Applied to the Study of ARHL and NIHL

The main difference that can be foreseen between ARHL and NIHL is the location within the cochlea of the damaged OHCs: while in NIHL these are mainly concentrated on the cochlea segment corresponding to the 4 kHz frequency, in ARHL they are more uniformly distributed all along the cochlea, with a preferential location close to the higher frequencies. The ARHL and NIHL audiograms are very different (see Figs. 8.5 and 8.6) but the TEOAE signals can be indistinguishable in terms of REPRO and SNR. Sometimes, particularly for ARHL, the TEOAE signal analyzed through REPRO and SNR could be indistinguishable even from a normal TEOAE.

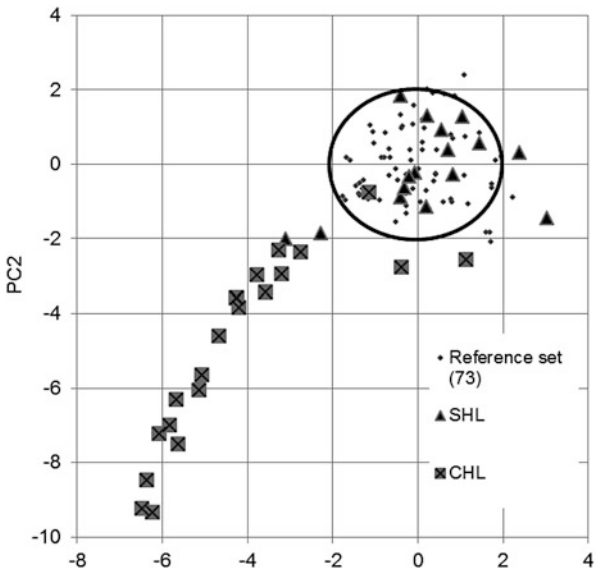

Fig. 8.15 TEOAE signals in the PC1/PC2 plane. *SHL*: signals from ears with sensorineural hearing losses; *CHL*: signals from ears with conductive hearing losses. Reproduced with permission [70]

RQA and RQA/PCA techniques were applied for studying noise-related hearing losses as well as age-related hearing losses, to look for possible early indication of the two types of damage. Figure 8.16 shows the recurrence plot of a TEOAE recorded from an NIHL (Fig. 8.16a) and from an ARHL subject (Fig. 8.16b). It has to be noted here that the chosen ARHL signal does not represent a severe condition (REPRO = 78). By comparing Fig. 8.16a with Fig. 8.8, it is clear that recurrence plot distinguishes between normal hearing and hearing losses, especially in terms of a reduction in the deterministic structure. On the other hand, Fig. 8.16b shows that the ARHL condition at the beginning stage could be indistinguishable even in the RQA plot from a normal condition. However, the reduction in determinism is confirmed from the mean values of the DET reckoned in different groups. In the three recurrence plots (Fig. 8.8 and in both panels of Fig. 8.16) the vertical and horizontal white bands reveal that transitions may have occurred; however the absence of fading to the upper left and lower right corners reveals that no trend or shift occurs.

Figure 8.17 reports the TEOAE signals recorded from NIHL ears as well as from normal ears in the PC1/PC2 plane. From the figure it can be noted that the NIHL signals fall in part within the normality circle and in part outside it, evidencing different levels of damage.

To quantify the amount of damage, a parameter, named RAD2D (two-dimensional radius), has been introduced. RAD2D measures the Euclidean distance between the origin of the PC1/PC2 plane and the position of the point representing a TEOAE signal in that plane [74, 75].

To evaluate the RAD2D values, the electronic model discussed in Sect. 8.7 was used, simulating increasing damages of the OHCs in the cochlea. A linear increase

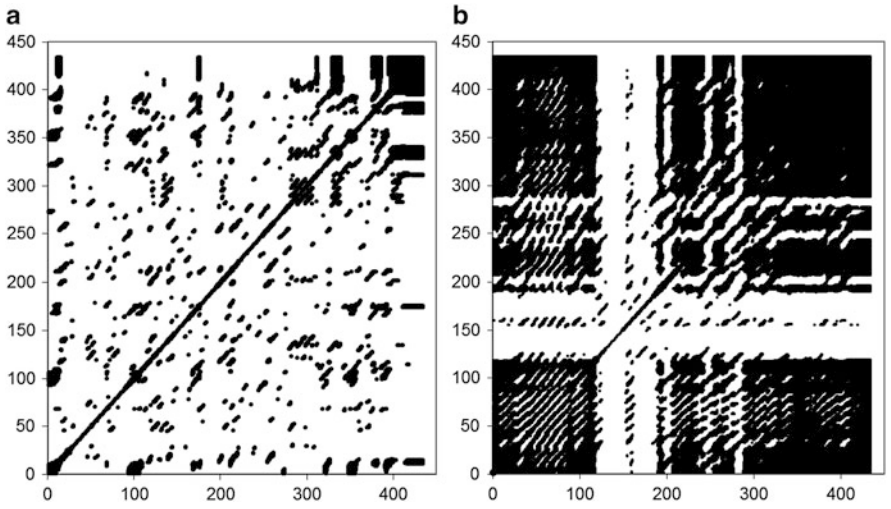

Fig. 8.16 Recurrence plot of a representative (**a**) NIHL (DET = 49.81) (**b**) ARHL TEOAE waveform (DET = 90.95)

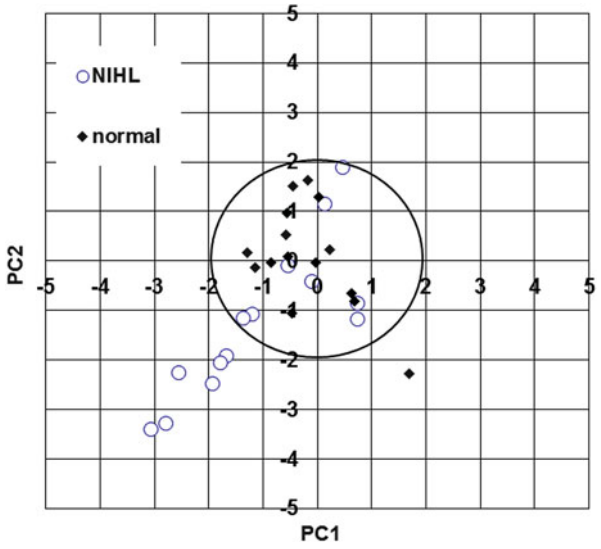

Fig. 8.17 TEOAE signals in the PC1/PC2 plane. *real_NIHL* represent ears with noise induced hearing losses; *real_Normal* represent normoacoustic ears

of the RAD2D with the amount of simulated damage was found [74]. Moreover, it is interesting to note that the RAD2D value obtained by the simulation of a normal ear (equal to 0.20) was close to the value of 0.21 obtained as the mean value from 15 TEOAE signals recorded in normal ears [74].

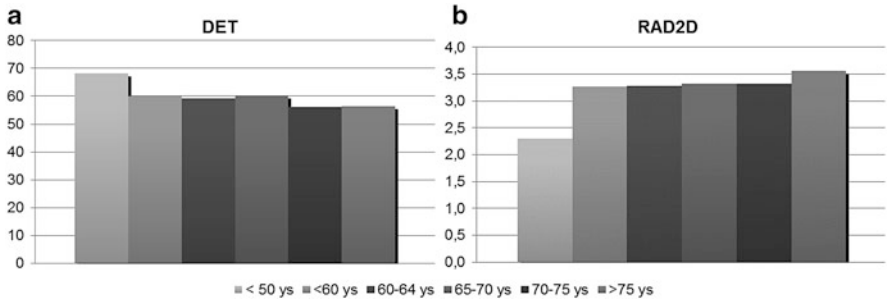

Fig. 8.18 (**a**) DET and (**b**) RAD2D values for five age-groups of ARHL ears. Adapted from [76]

A comparison was conducted among TEOAE signals recorded from three different groups: normoacoustic ears (Norm), ears with ARHL, and ears with NIHL centered at 4 kHz [76]. ARHL was defined if the subject was older than 50 years-old and presented at the PTA examination a threshold at 8 kHz higher than that at 4 kHz, and the threshold at 4 kHz higher than that at 2 kHz. From the RQA study it came out that while REC was not statistically different among the three groups, DET and RAD2D were statistically different between the ARHL and NIHL groups, as well as between each of the two impaired-ear groups and the normal group [76]. It is interesting to note here that 36 signals out of 115 among the pathological ones scored a REPRO value higher than 70, i.e. they would have passed the standard clinical ILO test.

Sub-dividing the ARHL group according to the increasing age, five groups were defined: younger than 60, between 60 and 64, 65–70, 70–75, and older than 75 years-old (audiograms shown in Fig. 8.5). Figure 8.18 reports the DET values and the RAD2D values obtained in the five age groups, compared with the values obtained from the normal group. From the figure it can be supposed that DET decreases and RAD2D increases with age, showing a slow age-related effect. However, the small numbers of used signals do not allow obtaining statistically significant differences among the different groups [76].

8.9 Conclusions and Future Directions

In this chapter RQA was presented as a powerful method to study the characteristics of OAEs. While OAEs are essential in the diagnosis of hearing losses, the information they carry on are only partially exploited by the actual diagnosis tools.

RQA has been applied to TEOAE signal sometimes in combination with the PCA technique. In this case the RQA descriptors were projected into the PCA plane, identifying the different signals with a simple dot in that space. This very simple representation of the TEOAE waveform proved to be able to discriminate among different signals coming from different ears, to cluster signals coming from the same

ear but recorded at different times, to discriminate among adults and newborns and among different types of hearing losses, as conductive versus sensorineural or age-related versus noise-induced hearing losses.

The reported research shows that the proposed approach can be useful in screening of adults, in longitudinal studies, in studies devoted to the evaluation of the efficacy of new pharmacological treatments, in conservation programs devoted to presbycusis, and in protection programs devoted to noise induced hearing losses. Moreover, it shows that RQA and RQA/PCA can be successfully used to study TEOAE signals and could be the basis for the definition of new clinical protocols, which could work side by side with existing ones, improving the actual diagnosis capabilities. However, it must be said that the reported results are just examples of the RQA potentiality in this field of research, and that further work, as well as a broader confirmation of the reported results needs to be carried out.

Software

The software used for the RQA analysis, that generates Recurrence plots and other RQA utilities, was downloaded from http://homepages.luc.edu/~cwebber/.

References

1. J. Bronzino (ed.), *The Biomedical Engineering Handbook* (CRC Press, Boca Raton, FL, USA 1995)
2. D.T. Kemp, Stimulated acoustic emissions from within the human auditory system. J. Acoust. Soc. Am. **64**(5), 1386–1391 (1978)
3. S. Hatzopoulos, J. Petrucelli, T. Morlet, A. Martini, Otoacoustic emission protocols revised. Data from adult subjects. Int. J. Audiol. **42**(6), 339–347 (2003)
4. C.A. Shera, J.J. Guinan Jr., Evoked otoacoustic emissions arise by two fundamentally different mechanisms: a taxonomy for mammalian OAEs. J. Acoust. Soc. Am. **105**, 782–798 (1999)
5. D. Konrad-Martin, D.H. Keefe, Time–frequency analysis of transient-evoked stimulus-frequency and distortion-product otoacoustic emissions: testing cochlear model predictions. J. Acoust. Soc. Am. **114**(4), 2021–2043 (2003)
6. W.E. Brownell, Outer hair cell electromotility and otoacoustic emissions. Ear Hear. **11**(2), 82–92 (1990)
7. R. Sisto, A. Moleti, Otoacoustic emissions and cochlear reflectivity. J. Acoust. Soc. Am. **124**(5), 2995–3008 (2008)
8. R.H. Withnell, C. Hazlewood, A. Knowlton, Reconciling the origin of the transient evoked otoacoustic emission in humans. J. Acoust. Soc. Am. **123**(1), 212–221 (2008)
9. S. Verhulst, J.M. Harte, T. Dau, Temporal suppression and augmentation of click-evoked otoacoustic emissions. Hear. Res. **246**, 23–35 (2008)
10. R. Probst, B.L. Lonsbury-Martin, G.K. Martin, A review of otoacoustic emissions. J. Acoust. Soc. Am. **89**(5), 2027–2067 (1991)
11. P. Avan, B. Buki, B. Maat, M. Dordain, H.P. Wit, Middle ear influence on otoacoustic emissions. I: non invasive investigation of the human transmission apparatus and comparison with model results. Hear. Res. **140**, 189–201 (2000)
12. P. Avan, P. Bonfils, Distortion-product otoacoustic emission spectra and high-resolution audiometry in noise-induced hearing loss. Hear. Res. **209**(1–2), 68–75 (2005)

13. A.L. Hamdan, K.S. Abouchacra, A.G. Al Hazzouri, G. Zaytoun, Transient-evoked otoacoustic emissions in a group of professional singers who have normal pure-tone hearing thresholds. Ear Hear. **29**(3), 360–377 (2008)
14. A.R. Fetoni, M. Garzaro, M. Ralli, V. Landolfo, M. Sensini, G. Pecorari, A. Mordente, G. Paludetti, C. Giordano, The monitoring role of otoacoustic emissions and oxidative stress markers in the protective effects of antioxidant administration in noise-exposed subjects: a pilot study. Med. Sci. Monit. **15**(11), PR 1–PR 8 (2009)
15. A. Paglialonga, S. Fiocchi, L. Del Bo, P. Ravazzani, G. Tognola, Quantitative analysis of cochlear active mechanisms in tinnitus subjects with normal hearing sensitivity: time–frequency analysis of transient evoked otoacoustic emissions and contralateral suppression. Auris Nasus Larynx **38**(1), 33–40 (2011)
16. World Health Organization (WHO). Deafness and hearing loss. Fact sheet N°300 (2013). http://www.who.int/mediacentre/factsheets/fs300/en/index.html. Accessed 21 July 2013
17. S. Stenfelt, Towards understanding the specifics of cochlear hearing loss: a modelling approach. Int. J. Audiol. **47**(S2), S10–S15 (2008)
18. G.A. Gates, J.H. Mills, Presbycusis. Lancet **366**(9491), 1111–1120 (2005)
19. EU-OSHA – European Agency for Safety and Health at Work. Combined exposure to Noise and Ototoxic Substances, 2009
20. H.F. Schuknecht, Presbycusis, in *Pathology of the Ear*, ed. by H.F. Schuknecht, M.R. Gacek (Harvard University Press, Cambridge, 1974)
21. H.F. Schuknecht, M.R. Gacek, Cochlear pathology in presbycusis. Ann. Otol. Rhinol. Laryngol. **102**(1 Pt 2), 1–16 (1993)
22. C.R. Jenning, N.S. Jones, Presbycusis. J. Laryngol. Otol. **115**(3), 171–178 (2001)
23. X.Z. Liu, D. Yan, Ageing and hearing loss. J. Pathol. **211**(2), 188–197 (2007)
24. K.K. Ohlemiller, M.E. Rybak Rice, J.M. Lett, P.M. Gagnon, Absence of strial melanin coincides with age-associated marginal cell loss and endocochlear potential decline. Hear. Res. **249**(1–2), 1–14 (2009)
25. E.C. Bielefeld, C. Tanaka, G.D. Chen, D. Henderson, Age-related hearing loss: is it a preventable condition? Hear. Res. **264**, 98–107 (2010)
26. Q. Huang, J. Tang, Age-related hearing loss or presbycusis. Eur. Arch. Otorhinolaryngol. **267**, 1179–1191 (2010)
27. A.R. Fetoni, P.M. Picciotti, G. Paludetti, D. Troiani, Pathogenesis of presbycusis in animal models: a review. Exp. Gerontol. **46**(6), 413–425 (2011)
28. OSHA United States Occupational Safety and Health Administration, 1910.95 CFR occupational noise exposure: hearing conservation amendment (final rule). Fed. Regist. **48**, 9738–9785 (1983)
29. EU-OSHA – European Agency for Safety and Health at Work. Noise in Figures, Risk Observatory Thematic Report, 2006
30. D. Henderson, E.C. Bielefeld, K.C. Harris, B.H. Hu, The role of oxidative stress in noise-induced hearing loss. Ear Hear. **27**(1), 1–19 (2006)
31. C.G. Le Prell, D. Yamashita, S.B. Minami, T. Yamasoba, J.M. Miller, Mechanisms of noise-induced hearing loss indicate multiple methods of prevention. Hear. Res. **226**, 22–43 (2007)
32. J.L. Puel, S. Saffiedine, C. Gervais d'Aldin, M. Eybalin, R. Pujol, Synaptic regeneration and functional recovery after excitotoxic injury in the guinea pig cochlea. C. R. Acad. Sci. III **318**(1), 67–75 (1995)
33. A.R. Fetoni, A. Ferraresi, C.L. Greca, D. Rizzo, B. Sergi, G. Tringali, R. Piacentini, D. Troiani, Antioxidant protection against acoustic trauma by coadministration of idebenone and vitamin E. Neuroreport **19**(3), 277–281 (2008)
34. A.R. Fetoni, R. Piacentini, A. Fiorita, G. Paludetti, D. Troiani, Water-soluble coenzyme Q(10) formulation (Q-ter) promotes outer hair cell survival in a guinea pig model of noise induced hearing loss (NIHL). Brain Res. **1257**, 108–116 (2008)
35. A.R. Fetoni, M. Ralli, B. Sergi, C. Parrilla, D. Troiani, G. Paludetti, Protective effects of *N*-acetylcysteine on noise induced hearing loss in guinea pigs. Acta Otorhinolaryngol. Ital. **29**(2), 70–75 (2009)

36. A.R. Fetoni, M. Ralli, B. Sergi, C. Parrilla, D. Troiani, G. Paludetti, Protective properties of antioxidant drugs in noise-induced hearing loss in the guinea pig. Audiol. Med. **6**(4), 271–277 (2009)
37. B.M. Vinck, P.B. van Cauwenberge, L. Leroy, P. Corthals, Sensitivity of transient evoked and distortion product otoacoustic emissions to the direct effects of noise on the human cochlea. Audiology **38**, 44–52 (1999)
38. Y. Uchida, T. Nakashimat, F. Ando, N. Niino, H. Shimokata, Is there a relevant effect of noise and smoking on hearing? A population-based aging study. Int. J. Audiol. **44**, 86–91 (2005)
39. D. Balatsouras, A. Kaberos, E. Karapantzos, E. Homsioglou, N.C. Economou, S. Korres, Correlation of transiently evoked otoacoustic emission measures to auditory thresholds. Med. Sci. Monit. **10**(2), MT24–MT30 (2004)
40. D. Davilis, S.G. Korres, D.G. Balatsouras, E. Gkoritsa, G. Stivaktakis, E. Ferekidis, The efficacy of transiently evoked otoacoustic emissions in the detection of middle-ear pathology. Med. Sci. Monit. **11**(12), MT75–MT78 (2005)
41. S. Hatzopoulos, A. Grzanka, A. Martini, W. Konopka, New clinical insights for transiently evoked otoacoustic emission protocols. Med. Sci. Monit. **15**(8), CR403–CR408 (2009)
42. M.L. Whitehead, B.B. Stagner, B. Lonsbury-Martin, G.K. Martin, Measurement of otoacoustic emissions for hearing assessment. IEEE Eng. Med. Biol. Mag. **13**, 210–226 (1994)
43. P. Ravazzani, F. Grandori, Evoked otoacoustic emissions: nonlinearities and response interpretation. IEEE Trans. Biomed. Eng. **40**(5), 500–504 (1993)
44. Otodynamic. ILO OAE Instrument User Manual. Issue 5a, 1997
45. C.A. Shera, Mechanisms of mammalian otoacoustic emission and their implications for the clinical utility of otoacoustic emissions. Ear Hear. **25**(2), 86–97 (2004)
46. J. Attias, M. Furst, V. Furman, I. Reshef, G. Horowitz, I. Bresloff, Noise-induced otoacoustic emission loss with or without hearing loss. Ear Hear. **16**(6), 612–618 (1995)
47. A. Shupak, D. Tal, Z. Sharoni, M. Oren, A. Ravid, H. Pratt, Otoacoustic emissions in early noise-induced hearing loss. Otol. Neurotol. **28**(6), 745–752 (2007)
48. M. Lucertini, A. Moleti, R. Sisto, On the detection of early cochlear damage by otoacoustic emission analysis. J. Acoust. Soc. Am. **111**(1–2), 972–978 (2002)
49. J.P. Zbilut, A. Giuliani, C.L. Webber, Recurrence quantification analysis and principal components in detection of short complex signals. Phys. Lett. A **237**, 131–135 (1998)
50. C. Manetti, M.A. Ceruso, A. Giuliani, C.L. Webber, J.P. Zbilut, Recurrence quantification analysis as a tool for characterization of molecular dynamics simulation. Phys. Rev. E **59**, 992–998 (1999)
51. G. Zimatore, A. Giuliani, C. Parlapiano, G. Grisanti, A. Colosimo, Revealing deterministic structures in click-evoked otoacoustic emissions. J. Appl. Phys. **88**(4), 1431–1437 (2000)
52. G. Zimatore, A. Giuliani, S. Hatzopoulos, A. Martini, A. Colosimo, Otoacoustic emissions at different click intensities: invariant and subject dependent features. J. Appl. Phys. **95**(6), 2299–2305 (2003)
53. P. Ravazzani, G. Tognola, M. Parazzini, F. Grandori, Principal component analysis as a method to facilitate fast detection of transient-evoked otoacoustic emissions. IEEE Trans. Biomed. Eng. **50**(2), 249–252 (2003)
54. W.A. Harrison, S.J. Norton, Characteristics of transient evoked otoacoustic emissions in normal-hearing and hearing impaired children. Ear Hear. **20**, 75–86 (1999)
55. A.B. Maxon, B.R. Vohr, K.R. White, Newborn hearing screening: comparison of a simplified otoacoustic emissions device (ILO1088) with the ILO88. Early Hum. Dev. **45**, 171–178 (1996)
56. T. Morlet, L. Goforth, L.J. Hood, C. Ferber, R. Duclaux, C.I. Berlin, Development of human cochlear active mechanism asymmetry: involvement of the medial olivocochlear system? Hear. Res. **134**, 153–162 (1999)
57. S.J. Norton, M.P. Gorga, J.E. Widen, R.C. Folsom, Y. Sininger, B. Cone-Wesson, B.R. Vohr, K. Mascher, K. Fletcher, Identification of neonatal hearing impairment: evaluation of transient evoked otoacoustic emission, distortion product otoacoustic emission, and auditory brain stem response test performance. Ear Hear. **21**(5), 508–528 (2000)

58. S.J. Norton, Application of transient evoked otoacoustic emissions to pediatric populations. Ear Hear. **14**, 64–73 (1993)
59. G. Zimatore, S. Hatzopoulos, A. Giuliani, A. Martini, A. Colosimo, Comparison of transient otoacoustic emission responses from neonatal and adult ears. J. Appl. Physiol. **92**(6), 2521–2528 (2002)
60. J.B. Allen, Nonlinear cochlear signal processing, in *Physiology of the Ear*, ed. by A.F. Jahn, J. Santos-Sacchi, 2nd edn. (Singular Thompson, San Diego, 2001), pp. 393–442
61. L. Robles, M.A. Ruggero, Mechanics of the mammalian cochlea. Physiol. Rev. **81**, 1305–1352 (2001)
62. H.P. Wit, P. van Dijk, P. Avan, Wavelet analysis of real ear and synthesized click-evoked otoacoustic emissions. Hear. Res. **73**, 141–147 (1994)
63. R.F. Lyon, C. Mead, An analog electronic cochlea. IEEE Trans. Acoust. Speech Signal Process. **36**(7), 1119–1134 (1988)
64. J. Merhaud, *Theory of Electroacoustics* (McGraw-Hill, New York, 1981)
65. C. Giguère, P.C. Woodland, A computational model of the auditory periphery for speech and hearing research. I. Ascending path. J. Acoust. Soc. Am. **95**(1), 331–342 (1994)
66. C. Giguère, P.C. Woodland, A computational model of the auditory periphery for speech and hearing research. II. Descending paths. J. Acoust. Soc. Am. **95**(1), 343–349 (1994)
67. G. Zimatore, M. Cavagnaro, A. Giuliani, A. Colosimo, Reproducing cochlear signals by a minimal electroacoustic model. Open J. Biophys. **2**, 33–39 (2012)
68. M.B. Gardner, M.S. Hawley, Network representations of the external ear. J. Acoust. Soc. Am. **52**, 1620–1628 (1972)
69. M.E. Lutman, A.M. Martin, Development of an electroacoustic analogue model of the middle ear and acoustic reflex. J. Sound Vib. **64**(1), 133–157 (1979)
70. G. Zimatore, M. Cavagnaro, A. Giuliani, A. Colosimo, Human acoustic fingerprints. Biophys. Bioeng. Lett. **1**(2) (2008)
71. L. Zheng, Y.T. Zhang, F.S. Yang, D.T. Ye, Synthesis and decomposition of transient-evoked otoacoustic emissions based on an active auditory model. IEEE Trans. Biomed. Eng. **46**(9), 1098–1106 (1999)
72. R. Sisto, A. Moleti, On the frequency dependence of the otoacoustic emission latency in hypoacoustic and normal ears. J. Acoust. Soc. Am. **111**, 297–308 (2002)
73. G. Tognola, F. Grandori, P. Avan, P. Ravazzani, P. Bonfils, Frequency-specific Information from click evoked otoacoustic emissions in noise-induced hearing loss. Audiology **38**(5), 243–250 (1999)
74. G. Zimatore, A.R. Fetoni, G. Paludetti, M. Cavagnaro, M.V. Podda, D. Troiani, Post-processing analysis of transient-evoked otoacoustic emissions to detect 4 kHz-notch hearing impairment – a pilot study. Med. Sci. Monit. **17**(6), MT41–MT49 (2011)
75. G. Zimatore, D. Stanzial, M.P. Orlando, Otoacoustic emissions, in *Acoustic Emission – Research and Applications*, ed. by W. Sikorski (InTech, Rijeka, 2013), pp. 203–223
76. G. Zimatore, Noise ad aging effects in otoacoustic emissions. Ph.D. Dissertation, Catholic University Medical School "A. Gemelli" of Rome Italy, 2012